SEISMIC BEHAVIOR OF A MASONRY CHIMNEY RETROFITTED WITH COMPOSITE MATERIALS: A PRELIMINARY APROACH

D. BRU, S. IVORRA & F. J. BAEZA
Civil Engineering Department, University of Alicante, Spain.

ABSTRACT

This paper presents a structural analysis of a masonry chimney, which is being catalogued as local interest heritage, according Eurocode 8. The chimney, located in Alicante (Spain), is severely damaged, and it shows several longitudinal cracks, and mortar loss between bricks. In order to guarantee the structural safety under seismic forces, the chimney was retrofitted with composite materials. This reinforcement comprised an internal textile reinforced mortar (TRM) layer, i.e. glass fiber mesh and cement matrix, and local reinforcement with longitudinal carbon fiber bands. This study consisted of two stages: first, numerical and experimental analyses of the original chimney were done. Second, design of an internal reinforcement scheme was done. The experimental text includes acceleration measures under ambient vibration for an operational modal analysis. And laboratory test for bricks and mortar to study the mineralogical composition and mechanical properties. The numerical analysis includes, preliminary pushover analysis before and after the reinforcement was done, and second, linear response spectrum analysis to evaluate the structural stability under the seismic demand.
Keywords: FEM, Reinforced masonry TRM walls, seismic loads, seismic retrofitting, slender masonry structures

1 INTRODUCTION

The recent Lorca earthquake increased the interest in the seismic behavior of masonry structures in Spain. In particular, the focus of the present paper is on the seismic behavior improvement of slender historical masonry constructions [1]. Nowadays, the existing literature related to the numerical analysis of chimneys is rather scarce. Some recent and insightful 3D nonlinear analyses of a collapsed reinforced concrete chimney were presented in Huang *et al*. [2]. Regarding to masonry chimneys, numerical results were presented by Pallarés, Ivorra, Lourenço and Foti ([3–5]). Moreover, a critical comparison between nonlinear static and dynamic analysis methods is presented with reference to a stone masonry minaret [6]. About the structural characterization of masonry chimneys and experimental test, different examples were presented in Aoki *et al*. (2006) [7] and Pallarés *et al*. (2009) [8]. This researches show the experimental vibration mode shapes and the relationship between the natural frequencies and the stiffness of the structure.

The present paper is focused on the analysis of a 25 m tall masonry chimney located in Agost (Alicante, Spain), Fig. 1. The chimney was built in the beginning of the 20th century in the service of a brick factory. The main objective of this research is to analyze the seismic vulnerability of the structure before and after the reinforcing process, according to Eurocode 8 [9] and NCSE Spanish [10] standard. Both linear and nonlinear pushover analyses were developed [11], for the unreinforced and reinforced structure. This reinforcement comprised an internal textile reinforced mortar (TRM) layer, i.e. glass fiber mesh and cement matrix, and local reinforcement with longitudinal carbon fiber composites.

2 GEOMETRY AND EXPERIMENTAL TESTS

2.1 Geometrical properties

The chimney was built in masonry bricks (24x11.5x5 cm), with mortar joints (1.50 cm), for a total height of 24.70 m. It can be divided in three different parts: 2.84x2.84 m squared section base with 0.80 m thickness; and the stack and crown, both with a regular octagonal cross section with variable dimensions and thickness (from 0.6 m at the stack-base connection to 0.25 m at the crown). The main characteristics of this structure are the drift of the top of the shaft and the longitudinal crack on the central part of the chimney, Fig. 1. Nowadays, the top of the shaft has a slope of 3%, besides the 10 m of longitudinal crack in the shaft of the chimney that shows the lack of cohesion between masonry bricks.

2.2 Laboratory tests

A survey campaign was carried out to estimate the chemical and physical properties of the masonry materials (bricks and mortars). Twelve samples were taken from the structure at
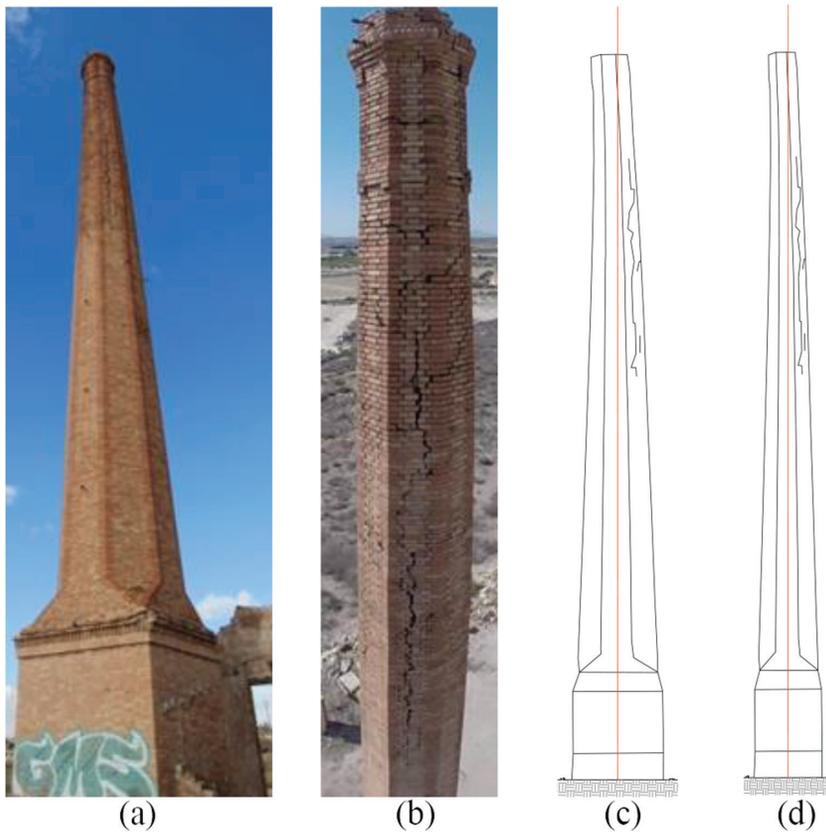

Figure 1: a) General view of the chimney, b) vertical cracking pattern along the stack, c) and d) NE and SE elevations.

different positions. Samples number M1, M2 and M6 were taken from the inner part of the chimney. All samples were analyzed using scanning optical microscopy technique and X-ray diffraction. The results showed a high concentration of sulphur in the interior of the chimney, Fig. 2, due to combustion processes during the industrial activity of the facility. This fact caused significant mortar and brick deterioration due to the acid action of the sulphur, if water was present because vapor condensation. The mortar was a lime mortar with silica sand, as showed the X-ray diffraction results included in Table 1.

Finally, mechanical and physical properties were analyzed. In particular, density and compression strength for mortars and bricks were measured, according to Magalhães
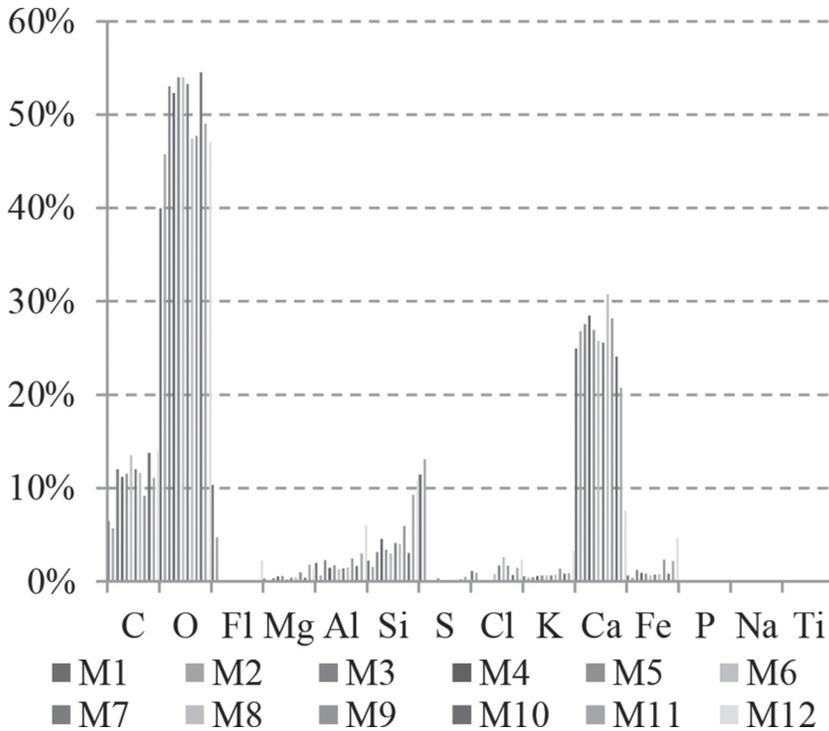

Figure 2: Results of SEM analysis.

Table 1: Results of DRX analysis.

| Samples | Crystalline phases | | | | |
	Gympsum ($CaSO_4 \cdot 2H_2O$)	Quartz (SiO_2)	Anhydrite ($CaSO_4$)	Calcite ($CaCO_3$)	Dolomite ($CaMgCO_3$)
M1	8.05%	14.10%	75.94%		
M3		28.97%		59.76%	6.85%
M6	14.22%	25.55%		60.23%	
M8		28.67%		67.58%	
M12	34.43%	19.53%		46.04%	

research [12]. The average density was equal to 1893 kg/m³ for the mortar and 2018 kg/m³ for the bricks. Moreover, the average compression strength for mortar was equal to 7.63 MPa and 37.79 MPa for brick. According to Eurocode 6 [13], for masonry walls, the compression strength was equal to 11.16 MPa, the tensile strength was equal to 0.2 MPa and the shear initial strength was equal to 0.2 MPa. Finally, the described survey ensures a KL1 knowledge level, according to Eurocode 8, leading to a confidence factor CF_{KL1}, 1.35.

2.3 General properties of the repair process

The reinforcement of the structure has been divided into several phases. First, the most damaged areas of mortar were repaired, i.e. all joints were cleaned with compressed air and damaged joints were completely removed. In the second phase, these damaged joints were repaired by means of new lime mortars, dosage 1/3 for slaked lime and 0–3 mm sand. In the third phase, the area where the cracks affected the whole wall thickness was repaired. In particular, all bricks near the crack were exchanged for new similar bricks and mortar.

After this preliminary repairing process of the masonry wall, the structural reinforcement was placed. The reinforcement comprised an internal textile reinforced mortar (TRM) and local reinforcement with longitudinal carbon fiber bands. In particular, one layer of fiberglass, Mapegrid G220, and Planitop Restauro mortar were placed together. Regarding the carbon fiber reinforcement, eight internal and longitudinal FRP bands – Carboplate E170/100/1.4 and E170/80/1.2 – were placed along the whole chimney. A special adhesive, specifically Adhesilex PG-1, guaranteed the bonding between the carbon fiber laminates and the repair mortar. MAPEI provided all referred materials.

2.4 Dynamic properties of the repair process

Ambient vibration tests were conducted on the chimney in June 2014 to assess the dynamic response at 12 different points only under ambient vibrations (Fig. 4). The structure was instrumented with eight 393B12 PCB Piezotronics uniaxial accelerometers, placed at 2, 10, 16 and 23.24 m from the structure's base, and connected to a centralized data acquisition system by means of long transducer cables. The accelerometers position and orientation are referred in Fig. 4, together with the experimental model used for OMA. Two PCB 482A22 signal
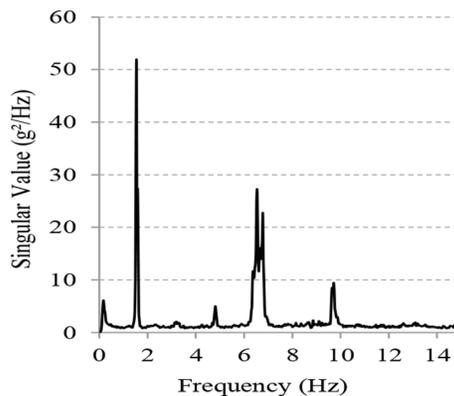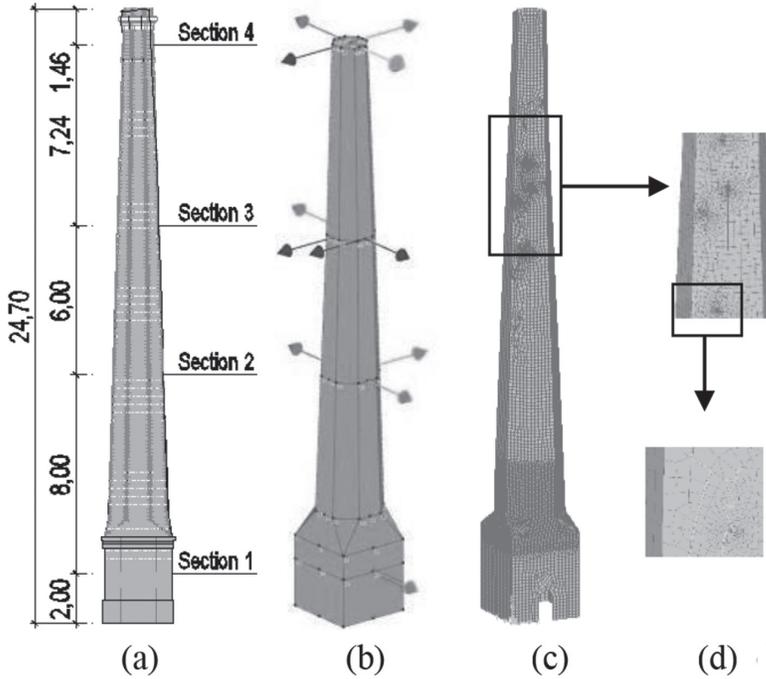

Figure 3: Natural frequencies of the mode shapes.

Figure 4: a) Position of the sensors, b) experimental model for OMA, c) numerical model for FEM, d) numerical model: Details of cracks.

conditioner and two Kyowa PCD 320 data logger registered the response during ambient vibration tests.

The measurement of the dynamic behavior of the structure was performed in two phases. In the first phase, eight accelerometers were used, and in the second phase, four of these were fixed as reference signals and the remaining four were moved between predefined positions and directions. In each setup, a continuous signal acquisition was carried out for approximately 10 min, with 100 Hz sampling frequency. Figure 5 shows the four vibration mode
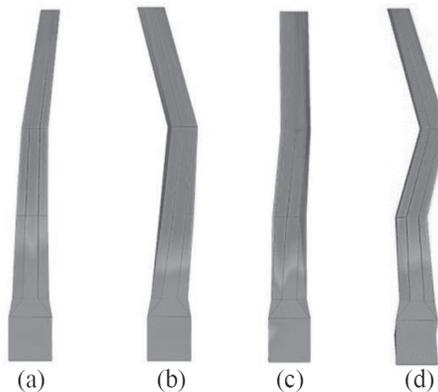

Figure 5: Modal shapes estimated from experimental tests: a) mode 1, b) mode 2, c) mode 3, and d) mode 4.

shapes estimated from the recorded measurements. The natural frequencies for these modes were 1.55Hz, 4.81Hz, 6.83Hz and 9.98Hz. All modes were detected in two orthogonal directions.

3 NUMERICAL MODEL

Two different numerical models were considered to evaluate the structural behavior of the masonry chimney. Both models use the Finite Element Method by means of the SAP2000 software [14], and they were modeled using four nodes shell elements. The main difference between the two models is that the first one considered the main crack in the chimney and the second model presented the reinforced structure, Fig. 4. The first model had a total 2543 nodes and 2538 shell elements. The second model had a total 15249 nodes and 14936 shell elements. In the model definition, the structural footing was considered fixed, the masonry weight per unit volume equal to 14.49 kN/m³, a constant Poisson's ratio equal to 0.25, and isotropic behavior was assumed for the whole chimney.

The material nonlinearities for masonry were reproduced by means of a multi-directional elastic and plastic curve. The compressive strength was estimated using the mean value 4.59 MPa obtained from experimental tests on masonry units and considering a safety factor. The behavior for compression curve was elastic with an initial stiffness of 3654 MPa up to a 4.59 MPa stress, and perfect plasticity afterwards. The reinforcement material is considered linear for tension and zero for compression.

After the analyses, the natural frequencies of the unreinforced model were 1.46, 5.10, 7.47 and 10.11 Hz and for reinforced model were 1.66, 5.93, 10.72, and 11.88 Hz.

4 RESPONSE SPECTRUM ANALYSIS

4.1 Elastic response spectrum

Seismic evaluation of the masonry chimney was done according to Eurocode 8 by means of a response spectrum analysis. Elastic response spectrum, for a 5% damping factor and special relevance region, has been calculated with the Spanish standard NCSE 02, Fig. 6. The constant acceleration part of the spectrum was located between 0.13 s and 0.54 s periods. A type II ground was selected according to geotechnical parameters and preliminary excavation near the foundation of the chimney. The results of the excavation showed that the first 1.5 m of the excavation was natural loose ground, and from 1.5 m to 2.25 m of the excavation, were sandy loams with good consistency. According to the ground properties, basic acceleration and maximum acceleration values are equal to 0.11 g and 0.15 g.

Figure 6 shows the natural periods for unreinforced and reinforced structures. In particular, seismic acceleration, for the first mode of vibration, increases by 11.33% for reinforced structure. However, seismic acceleration decreases by 10% for the fourth vibration mode and remains constant for the second mode of vibration. These results show that a high structural reinforcement may reduce the seismic demand, although the actions for the first mode were increased.

Finally, ultimate limit state verification for bending and shear has been done by means of the Eurocode 8. In particular, ultimate bending moment before the structural collapse has been evaluated as the overturning stability. This moment was calculated by equilibrium with the compressive stress resultant of the masonry section, with maximum compressive strain equal to 0.35%, and the tensile stress resultant of the reinforced area, with maximum tensile
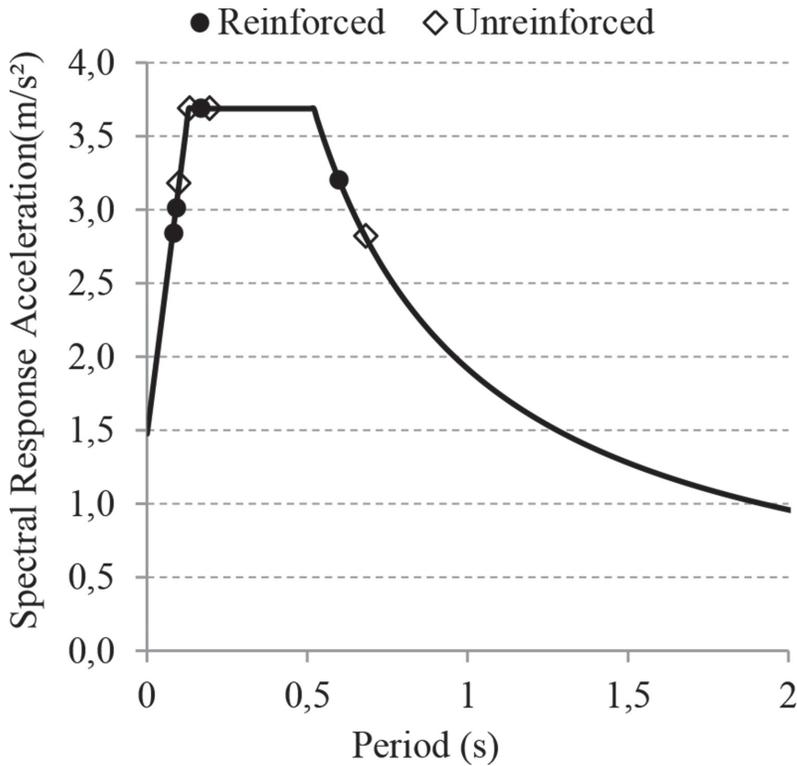
Figure 6: Elastic response spectrum.

strain equal to 1%. Furthermore, shear capacity of the masonry section was assessed by means of the Mohr-Coulomb criteria, with cohesion equal to 0.2 MPa and friction coefficient equal to 0.4.

Figure 7 shows the bending results for linear analysis and bending resistance moment for reinforced and unreinforced structure. Before reinforcement of the structure, the masonry chimney shows high risk of bending collapse. However, for the reinforced chimney, all bending moments of the seismic actions are lower than the bending capacity of the reinforced sections. Furthermore, in case of shear seismic actions, Fig. 8 shows similar conclusions than bending analysis. In particular, the critical region is the upper 10 m of the masonry chimney.

5 PUSHOVER ANALYSIS

In order to analyze the nonlinear response of the system versus the seismic actions, a modal pushover analysis (MPA) was done. In this case, nonlinear response was considered for mode 1 and linear response for higher modes, according to Chopra *et al.* 2002 [11]. The basic idea of MPA is to combine the results of N pushover analyses, the nth of which is based on the invariant forces distribution proportional to the effective mass and modal shape, Equation 1.

$$s_n = M \cdot \Phi_n \tag{1}$$

where M = modal mass; Φ_n = n^{th} elastic mode shape.; and s_n = invariant force distribution for mode n.
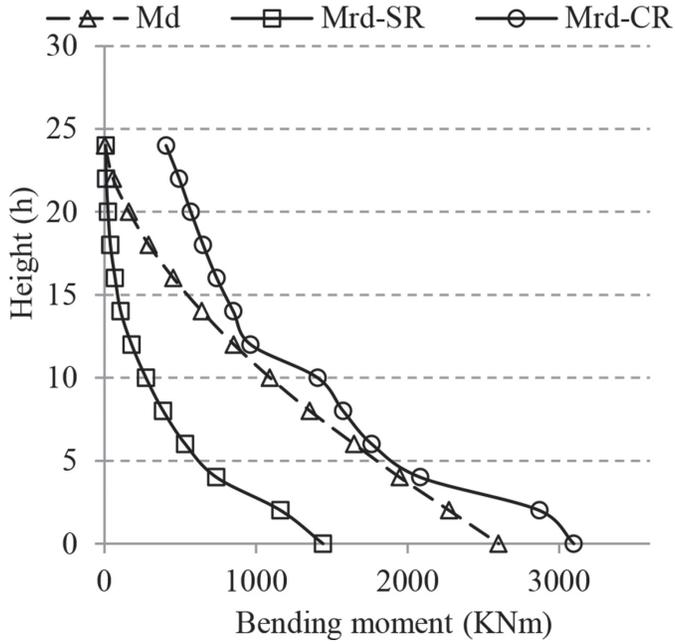
Figure 7: Linear analysis results: Computed bending moment diagrams (Md); Moment resistance without reinforcement (Mrd-Sr); Moment resistance with reinforcement (Mrd-CR).
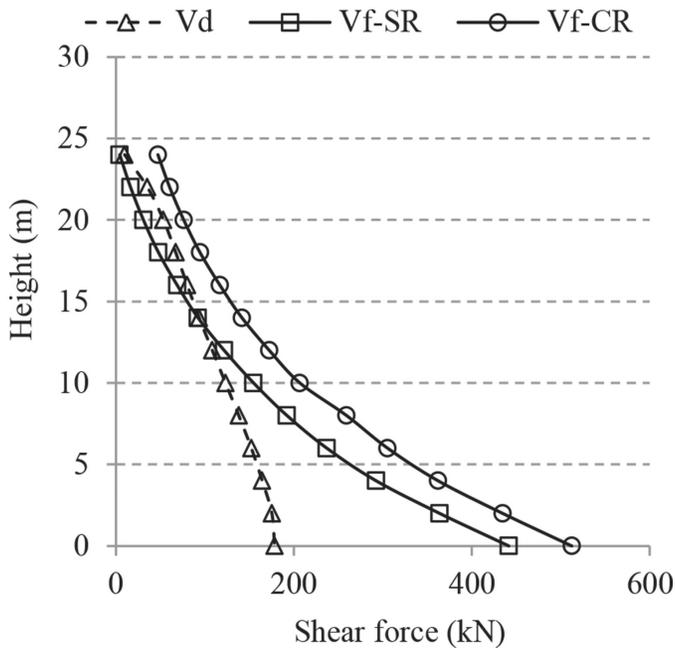

Figure 8: Linear analysis results: Computed shear force diagram (Vd); Shear resistance without reinforcement (Vf-SR); Shear resistance with reinforcement (Vf-CR).

Figure 9 shows the capacity curve for reinforced and unreinforced first mode of vibration. The collapse point (CP), shows the maximum displacement, before the structure collapse due to the second-order effects. This failure mode is characterized by the cracking of the upper zone of the stack, Fig. 10, reaching the minimum value of the compression area, which prevents the collapse of the structure. Moreover, this failure mode shows that the structure has a small resistance capacity as cracked structure. The maximum displacement is seven times greater than the elastic displacement.

Furthermore, Fig. 9 shows that the stiffness of the cracked chimney and the maximum displacement for the reinforced structure are bigger than the unreinforced structure. In particular, the cracked stiffness of the reinforced structure is 1.45 times higher than unreinforced chimney. Moreover, reinforced structure shows a new crack pattern compared with unreinforced structure, Fig. 10. This new pattern has much more cracks at the bottom of the stack.

Figure 11, shows the relationship between capacity and demand curve, for the reinforced structure in the ADSR system. In this case, the performance point (PP) is 0.15 m and 63.28 kN, Fig. 9, in the real capacity curve. The first result of the Fig. 11 is that the period of the cracked structure, T_{1NL}, is three times bigger than the elastic period for linear analysis, T_{1L}. Moreover, the base shear demand for nonlinear analysis is equal to 30% of the base shear for linear analysis.

Finally, Equation 2 allows to analyze the real effect of the highest modes of vibration. In particular, for lineal analysis, the maximum displacement for modes 2 and 4 are 3.59 mm and 0.74 mm. In other words, the higher mode contribution to maximum displacement of the structure is less than 10% of the full displacement. For this reason, if the ultimate limit state, according to Eurocode 8, depends on the maximum displacement of the structure, the effect
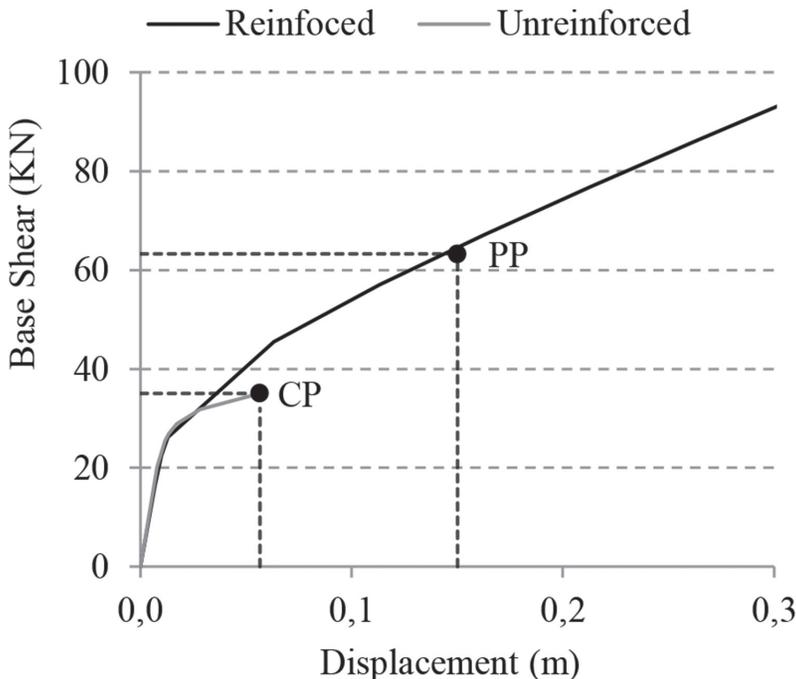

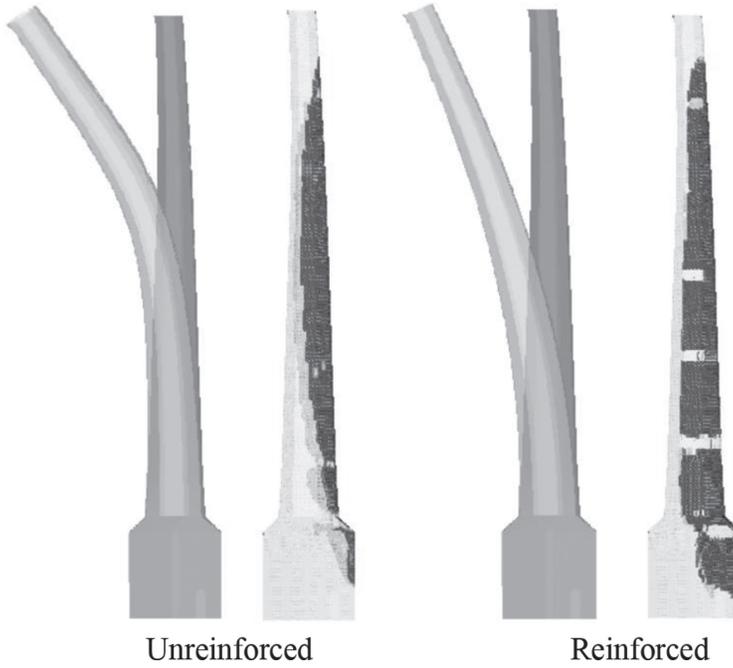Figure 9: Nonlinear capacity curve for the mode 1.

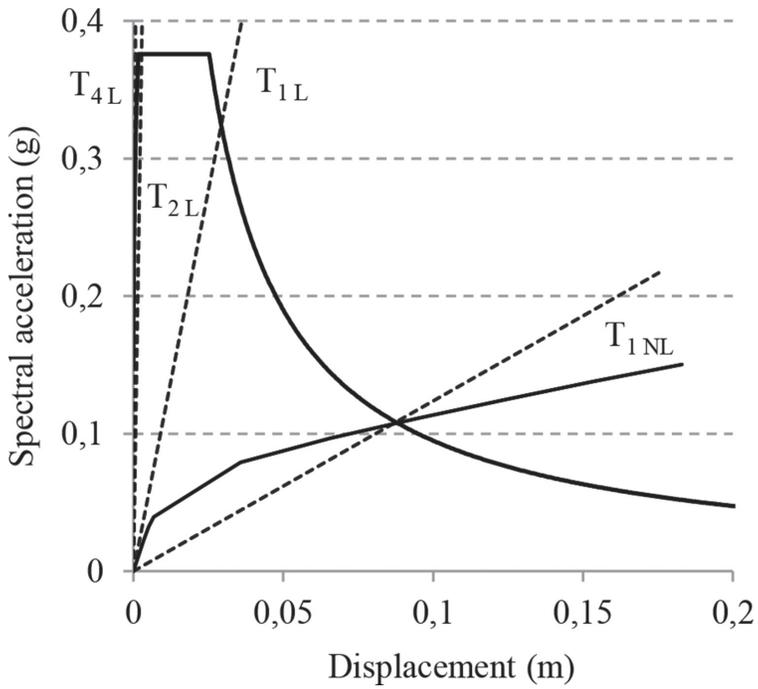Figure 10: Cracking patterns for failure of pushover mode 1.

Figure 11: ADSR demand and capacity spectrum.

of highest modes to the full displacement is less important than the first mode contribution in nonlinear analysis.

$$d_n = \frac{a_n}{w_n^2} \tag{2}$$

where d_n = modal displacement; a_n = spectral acceleration.; and w^2_n = natural frequency for mode n.

6 CONCLUSIONS

In this paper, a reinforcement scheme with composite materials was proposed for a 24.5m-high masonry chimney. This reinforcement comprised an internal textile reinforced mortar layer and local reinforcement with longitudinal carbon fiber bands. The results showed that the reinforcement prevents the structural collapse. Moreover, response spectrum analysis shows more seismic demand than pushover analysis, due to the effect of energy loss by cracking of the masonry chimney.

ACKNOWLEDGMENT

REFERENCES

[1] Magliulo, G., Ercolino, M., Petrone, C., Coppola, O. & Manfredi, G., The Emilia earthquake: seismic performance of precast reinforced concrete buildings. *Earthquake Spectra*, **30**(2), pp. 891–912, 2014.
https://doi.org/10.1193/091012eqs285m

[2] Huang, W. & Gould, P.L., 3-D pushover analysis of a collapsed reinforced concrete chimney. *Finite Elements in Analysis and Design*, **43**(11–12), pp. 879–887, 2007.
https://doi.org/10.1016/j.finel.2007.05.005

[3] Pallarés, F.J., Ivorra, S., Pallarés, L. & Adam, J.M., State of the art of industrial masonry chimneys: a review from construction to strengthening. *Construction and Building Materials*, **25**(12), 4351–4361, 2011.
https://doi.org/10.1016/j.conbuildmat.2011.02.004

[4] Lourenço, P.B., Recommendations for restoration of ancient buildings and the survival of a masonry chimney. *Construction and Building Materials*, **20**(4), pp. 239–251, 2006.
https://doi.org/10.1016/j.conbuildmat.2005.08.026

[5] Foti, D., Dynamic identification techniques to numerically detect the structural damage. *The Open Construction and Building Technology Journal*, **7**(1), pp. 43–50, 2013.
https://doi.org/10.2174/1874836801307010043

[6] Peña, F., Lourenço, P.B., Mendes, N. & Oliveira, D.V., Numerical models for the seismic assessment of an old masonry tower. *Engineering Structures*, **32**(5), pp. 1466–1478, 2010.
https://doi.org/10.1016/j.engstruct.2010.01.027

[7] Aoki, T. & Sabia, D., Structural characterization of brick chimney by experimental tests and numerical model updating. *Masonry International*, **19**, pp. 41–52, 2006.

[8] Pallarés, F.J., Ivorra, S., Pallarés, L. & Adam, J.M., Seismic assessment of a CFRP-strengthened masonry chimney. *Proceedings of the Institution of Civil Engineers - Structures and Buildings*, **162**(5), pp. 291–299, 2009.
https://doi.org/10.1680/stbu.2009.162.5.291

[9] European Commitee for Standardization, Eurocode 8: Design of structures for earthquake resistance - Part 1 : General rules, seismic actions and rules for buildings. *European Committee for Standardization*, **1**(1), 2004.

[10] Ministerio de Fomento. Gobierno de España, "Norma de construcción sismorresistente: Parte general y edificación (NCSE-02)," *Real Decreto 997/2002, de 27 de Septiembre de 2002*. 2002.

[11] Chopra, A.K. & Goel, R.K., A modal pushover analysis procedure for estimating seismic demands for buildings. *Earthquake Engineering & Structural Dynamics*, **31**(3), pp. 561–582, 2002.
https://doi.org/10.1002/eqe.144

[12] Magalhães, A. & Veiga, R., Physical and mechanical characterisation of historic mortars. Application to the evaluation of the state of conservation [Caracterización física y mecánica de los morteros antiguos. Aplicación a la evaluación del estado de conservación]. *Materiales de Construcción*, **59**(295), pp. 61–77, 2009.
https://doi.org/10.3989/mc.2009.41907

[13] C. E. De Normalisation, "EN 1996-1-1:1995 Eurocode 6 - Design of masonry structures - Part 1-1: General rules for reinforced and unreinforced masonry structures," *Management*, pp. 1–123, 2005.

[14] CSI, "SAP2000. Analysis Reference Manual," *CSI: Berkeley (CA, USA): Computers and Structures INC*. p. 496, 2016.